Available online at www.sciencedirect.com
ScienceDirect
Journal of the European Ceramic Society 30 (2010) 1903–1909
www.elsevier.com/locate/jeurceramsoc

Stability of rare earth oxides in a moist environment at high temperatures—Experimental and thermodynamic studies. Part I: The way to assess thermodynamic parameters from volatilisation rates

Emilie Courcot [a,*], Francis Rebillat [a,*], Francis Teyssandier [a], Caroline Louchet-Pouillerie [b]

[a] *Université de Bordeaux, Laboratoire des Composites ThermoStructuraux, 3 Allée de la Boétie, 33600 Pessac, France*
[b] *Snecma Propulsion Solide, Groupe SAFRAN, ZI Les Cinq Chemins, 33185 Le Haillan, France*

Received 7 July 2009; received in revised form 4 February 2010; accepted 8 February 2010
Available online 17 March 2010

Abstract

A methodology based on a weight loss measurement was used to quantify the volatility of yttria in high temperature water vapor. This method was first assessed on silica. Sintered materials with a shape of pellets were exposed at temperatures between 1000 and 1400 °C in air with 50 kPa of water at atmospheric pressure, under a flowing gas velocity of 5 cm s^{-1}. Besides the volatilisation rate, the nature of the volatile gaseous species was determined using a kinetic study. Knowing the nature of flows in the furnace, partial pressures of yttrium (oxy-)hydroxide in equilibrium over Y_2O_3 were calculated, and used to assess the enthalpies of formation of YO(OH) and $Y(OH)_3$.

Keywords: Corrosion; SiO_2; Y_2O_3; Refractories; Thermodynamics

1. Introduction

Materials including rare earth oxides, and especially Y_2O_3, are more and more used in high temperature applications. For example, YSZ (ZrO_2–8% Y_2O_3) is employed as an electrolyte in SOFCs.[1] Such an electrolyte can be in contact with a moist or oxidizing environment along one of its interfaces with an electrode. Here, the volatilisation of yttria can have a few negative effects: the ionic conductivity can decrease, and an allotropic transformation can occur with the departure of the stabilizing element of the cubic ZrO_2 phase. Elsewhere, thermal and/or environmental barrier coatings can contain Y_2O_3 in their compositions: YSZ (ZrO_2–8% Y_2O_3),[2] YAG ($Y_3Al_5O_{12}$)[3] and yttrium silicates.[4] In this latter case, yttria volatility generates porosity and leads to a permeable coating less efficient against diffusion of oxidizing species. Moreover, when Y_2O_3 is used as a sintering agent of Si_3N_4,[5] $Y_2Si_2O_7$ is formed along grain boundaries. During corrosion, a decreasing of mechanical properties should occur with the loss of cohesion between grains.

In the above-described applications, materials have to resist at high temperatures (>1000 °C) under a moist environment. Moisture provokes a degradation of materials through a corrosion process. By reaction of water with the oxides, volatile hydroxides $M(OH)_x$ or oxy-hydroxides $MO_y(OH)_z$ are formed (Eq. (1)).

$$\text{Oxide (s, l)} + H_2O\,(g) \rightarrow \text{hydroxide (g) or oxy-hydroxide (g)} \quad (1)$$

Hydroxide species play a key role in the high temperature reactivity of refractory materials in moist environments. In order to predict the behaviour of these materials and particularly their vaporization rate, the thermodynamic properties of hydroxide species have to be accurately known. These data can be determined from the measurement of partial pressures of gaseous species in equilibrium with the studied material, since they represent the maximum quantities of materials able to be removed. The flow conditions of corrosive and oxidizing species around the material have to be known to correctly estimate the volatili-

* Corresponding authors. Tel.: +33 556 84 47 39; fax: +33 556 84 12 25.
E-mail addresses: courcot@lcts.u-bordeaux1.fr (E. Courcot), rebillat@lcts.u-bordeaux1.fr (F. Rebillat).

0955-2219/$ – see front matter © 2010 Elsevier Ltd. All rights reserved.
doi:10.1016/j.jeurceramsoc.2010.02.011

sation rate of a material. Then, it is possible to deduce its ageing velocity and its maximal life duration. However, these calculations can only be done if all the thermodynamic parameters are already known. As far as our knowledge, the corrosion process of Y_2O_3 has not yet been studied and the thermodynamic data of the gaseous volatile species formed at high temperatures in moist environment are unknown.

In this work, it is proposed to assess the Gibbs free energy of formation of yttrium hydroxides or oxy-hydroxide by studying the volatilisation of Y_2O_3 at high temperatures in moist environment at atmospheric pressure.

2. Bibliographic data

The formation of gaseous metal hydroxides over a metal oxide requires oxidizing and corrosive environments at high temperatures. The determination of hydroxide partial pressures in equilibrium with the metal oxide can be done with three methods: the Knudsen cell, the transpiration method and the weight loss measurement.

With respect to the Knudsen cell, the nature of the gaseous species in equilibrium with the oxide, as well as their partial pressures, are determined with a mass spectrometer. This method is restricted to low partial pressures as the ionizer and detector of the instrument cannot tolerate $P(H_2O)$ greater than 1 Pa. In this method, reducing gaseous environments are generally required. The Knudsen cell technique must be adapted for water vapor studies: alternatively H_2 (g) may be introduced to react with the oxide to form H_2O (g) and the metal hydroxides. Moreover, only gaseous species, which do not condensate below 300 °C, can be detected and quantified. For example, with this technique, Meschi and his colleagues studied the reactions between B_2O_3 and H_2O and between Li_2O and H_2O.[6,7] Murad measured the thermochemical properties of gaseous FeO and FeOH.[8] More recently, Hildenbrand and Lau used this technique to study the silicon hydroxides[9,10] and the manganese oxides and hydroxides.[11]

The transpiration method is another valuable quantitative technique for obtaining data on hydroxides formation: a carrier gas transports a vapor at equilibrium towards a cold part of device where hydroxides condense. The amount of condensed material is accurately determined by an appropriate analytical technique. From the amount of condensate, the vapor pressure of that species can be calculated. This vapor pressure calculated as a function of water vapor pressure to confirm the species identity and as function of temperature to obtain thermodynamic data. For example, Hashimoto used this technique to study the formation of Ca, Si and Al hydroxides.[12] More recently, this transpiration method was used to study the equilibrium of $Ba(OH)_2$ over BaO,[13] and Si hydroxides over SiO_2.[14]

Further, a weight loss measurement can be used to access to partial pressure values. The weight change obtained from initial and final weights is used to calculate the partial pressure of volatile species. For example, Opila and Myers studied with this methodology the alumina volatility in water vapor at elevated temperatures ($P(H_2O) = [15–68\ kPa]$, $P_{tot} = 100\ kPa$, $T = [1250–1500\ °C]$, $v_{gas} = 4.4\ cm\ s^{-1}$).[15] Here, knowing that the hydroxide partial pressures depend on the water vapor partial pressure, the nature of volatile species is determined. The plot of log P(Al–OH) in function of log $P(H_2O)$ yields a slope of 1.5, which is in agreement with the value of the stoichiometric reaction ratio associated to H_2O in Eq. (2).

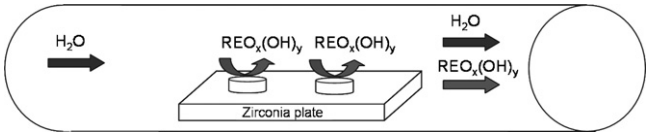

Fig. 1. Configuration of the pellets in the corrosion furnace.

$$\tfrac{1}{2}Al_2O_3 + \tfrac{3}{2}H_2O \rightarrow Al(OH)_3 \quad (2)$$

In this work, the last method was chosen to determine the Gibbs free energy of formation of yttrium hydroxides.

For that purpose, air saturated with a controlled amount of water vapor flowed over a pellet made of oxides that was disposed in a tubular furnace. The flow conditions of corrosive and oxidizing species around the material sample were controlled to provide a good estimation of the volatilisation rate.

3. Experimental procedure

In order to validate the experimental procedure, experiments were first realised on silica. Actually, silica was chosen because its behaviour under moist environment is well documented[4] and all the thermodynamic parameters about silicon hydroxides formations are already assessed.[16] Silica pellets (SiO_2, 99.8%, Chempur) were prepared as the other materials in this study, to always consider the same exchange surface area. Powders (SiO_2, 99.8%, Chempur and Y_2O_3, 99.9%, Chempur) were mixed and compacted under an unidirectional pressure of 0.5 MPa during 10 min. Pellets were heat treated at 1300 °C during 5 h under ambient air for desorption and sintering. The porosity was around 25%.

As mentioned in the literature, the assessment of thermodynamic data is allowed only when the partial pressures are able to be determined. This requires that the thermodynamic equilibrium is reached: the hydroxides formation rate is much higher than the evacuation one. The volatilisation experiments were carried out on oxide pellets ($\varnothing = 10$ mm, thickness ~ 2 mm, $S \sim 150\ mm^2$) in a corrosion furnace, whose principle is described elsewhere.[17] The conditions of corrosion are: temperatures between 1000 and 1400 °C, a moist air (water vapor partial pressure up to 65, 100 kPa total pressure with air to complete), with different gas velocities, during times between 1.5 and 25 h. Alumina furnace tube was used for the experiments due to its corrosion resistance at high temperatures. However, in moist environment, alumina can form $Al(OH)_3$ gaseous species that may react with the surface of the pellet and lead to formation of YAG ($Y_3Al_5O_{12}$) or YAM ($Y_4Al_2O_9$) from 1200 °C. To prevent as far as possible this pollution to occur, it was decided (i) to limit the experiment duration and (ii) to use a new pellet for each new experiment, and (iii) to dispose the pellet on a zirconia plate (Fig. 1). For the silica reference sample, no mullite formation was observed under such conditions. The limited aluminum

pollution was checked at the sample surface by use of various characterizations: X-ray diffraction, Raman spectroscopy and energy dispersive spectroscopy. Data were considered as accurate after similar results obtained from three independent experiments.

The weight loss induced by water corrosion was measured according to a reactive vaporization (Eq. (3)). It was well known that the gaseous hydroxide species should condensate at relatively high temperatures (upper than 300 °C).[9–14] Indeed, a white deposit is observed downstream from the samples inside the furnace. As it can be seen later, in the case of a porous pellet, allowing the production of large amount of hydroxides, it can be considered that their evacuation over the sample occurred by convection, through the geometric surface (the diffusion of hydroxides inside the porosities of this pellet is a fast phenomenon in regard to their evacuation by convection). Knowing the sample surface area in contact with the moist environment, the oxide volatilisation rate k_l was derived directly from the slope of the straight line representing the weight loss/surface ratio as a function of corrosion time.

$$M_aO_b + yH_2O \rightarrow aMO_x(OH)_y \quad \text{with } x = \frac{b+y}{a} - y \qquad (3)$$

In our working conditions, the moisture supply was very high compared to the consumed quantity, and further, the reaction kinetics being very slow, the low quantity of gaseous products was assumed to be easily evacuated far from the sample surface. Thus the volatilisation process was only limited by the surface reaction. From values of Reynolds numbers (equal to 45 at 1673 K), it has been first checked that the volatilisation process is mainly controlled by a convective flow through the furnace. Moreover, calculations of the involved gaseous flows show that the convection would limit the volatilisation process (in regard to the diffusion one). The hydroxide partial pressure over the oxide is thus deduced from the volatilisation rate (Eq. (4)).

$$k_l = v_{gas} \times 3.6 \times M_{M_aO_b} \times \frac{1}{a} \times \frac{P_{M-OH}}{R \times T_{amb}} \qquad (4)$$

where k_l is the volatilisation rate (mg cm^{-2} h^{-1}); v_{gas} is the gas flow velocity at room temperature (cm s^{-1}); $M_{M_aO_b}$ is the molar weight of M_aO_b (g mol^{-1}); a is the stoichiometry ratio before $MO_x(OH)_y$ in Eq. (3); P_{M-OH} is the sum of the volatile (oxy-)hydroxide partial pressures (Pa); R is the ideal gas constant (=8.314 J mol^{-1} K^{-1}); T_{amb} is the ambient temperature (296 K).

As the reactive volatilisation process is thermally activated, the Arrhenius law is used to fit the variations of the volatilisation rate as a function of temperature and to calculate the kinetic parameters (the activation energy E_a and the preexponential term k_0) of the hydroxide formation. Using Eq. (4), the average partial pressure of the hydroxide can thus be determined. At a given temperature, the Gibbs free energy of formation of the hydroxide is estimated using Gibbs free energy minimization technique.[18] Without specific mention, thermodynamic data used for these calculations come from the COACH database associated to the software. By running thermodynamic calculations using the parameters corresponding to the experimental

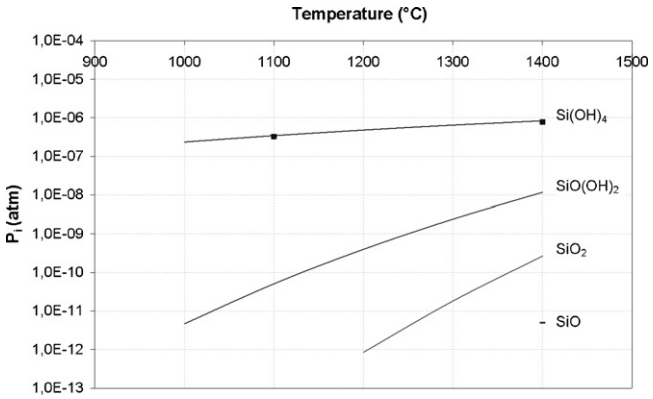

Fig. 2. Theoretical partial pressures of silicon hydroxides in function of temperature. Comparison with experiments: dots (50 kPa H_2O, at P_{atm} with v_{gas} = 5 cm s^{-1}).

conditions (temperature, total pressure and H_2O partial pressure), a value of the Gibbs free energy of formation of the hydroxide is selected in order to give the measured partial pressure. The repetition of this procedure for several temperatures allowed to establish the temperature dependence of the Gibbs free energy of formation of the hydroxide in the range from 1000 to 1400 °C.

4. Assessment of the method on silica

The whole procedure was checked with silica since its equilibrium properties between solid state and gaseous species in moist environment are already well known.[4] For temperatures ranging between 1000 and 1400 °C, $Si(OH)_4$ is by far the main gaseous silicon bearing species and partial pressures of $SiO(OH)_2$, SiO and SiO_2 were assumed to be negligible (Fig. 2). Fig. 3 shows the linear weight loss of silica that increases with temperature. Its slope corresponds to the volatilisation rate k_l of the solid oxide. These volatilisation rates appear one order of magnitude higher than those reported in literature.[19] This discrepancy can be explained by the nature of flows. Indeed, in many experiments,[19,20] the volatisation process is controlled by the diffusive flows and in these conditions, the volatilisation rate may be faster. Indeed, the equations allowing relating the k_l

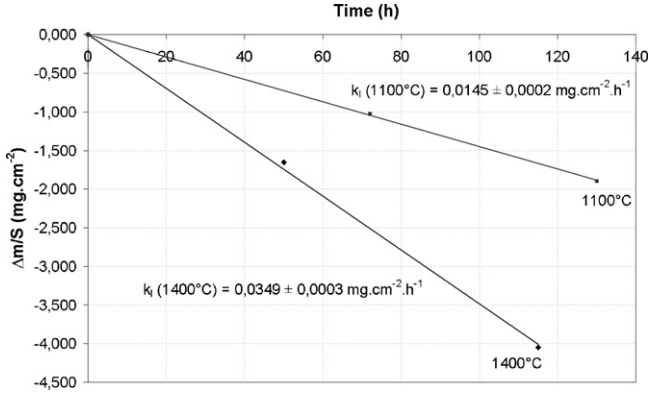

Fig. 3. Weight losses during volatilisation of SiO_2 at different temperatures (under corrosion at 50 kPa H_2O, at P_{atm} with v_{gas} = 5 cm s^{-1}).

rate to the hydroxides partial pressures are different. However each kind of experiment, in condition of thermodynamic equilibrium, the hydroxides partial pressures, over the solid surface, are always identical (this has been checked in our work, during the validation procedure, but not explained in a publication).

The volatilisation process is an interfacial phenomenon, thermally activated. The activation energy is thus deduced from the Arrhenius law. From these experiments, the estimated activation energy value around 56 kJ mol^{-1} is in good agreement with those in the literature (61 ± 8 kJ mol^{-1}).[12,19] The partial pressure of $Si(OH)_4$ is calculated from Eq. (4) and then compared with the partial pressure calculated by running minimization of the Gibbs free energy of the chemical system with parameters corresponding to the experimental parameters. The Gibbs free energy of formation of silicon hydroxides comes from ref. 16. A good agreement between experimental and calculated equilibrium hydroxide partial pressures over SiO_2 is therefore obtained (Fig. 2). The deviation between these two values is less than 10%. The experimental approach can be reasonably considered as accurate and the following main assumptions are validated: the environmental conditions used in the furnace allow thermodynamic equilibrium to be reached along the sample surface area, and the limiting step in the volatilisation process leads to equilibrium vapor by a mainly convective flow.

5. Reactive volatilisation of yttria

In order to assess the thermodynamic parameters of YOOH and $Y(OH)_3$, an overview of Y-containing gaseous and solid species has to be done and their associated thermodynamic data are compiled.

With regard to gaseous species, the vaporization of Y_2O_3 has already been studied in dry air by mass spectrometer coupled with a Knudsen cell. This method revealed the formation of YO, Y_2O, Y_2O_2. Though not experimentally observed, the existence of YO_2 molecule was deduced by analogy with rare earth compounds.[20–23] Their thermodynamic data were gathered in the COACH database.[18]

The most recent modelling of the yttrium–oxygen system was realised by Djurovic et al.[24] Contrary to the first thermodynamic evaluations of the Y–O system,[25–28] Djurovic et al. take into account the gaseous and liquid phases and the two polymorphic phases of Y and Y_2O_3. In the working temperatures ranging between 1000 and 1400 °C, α-Y_2O_3 (C-type Y_2O_3) is the most stable phase to consider in calculations (Eq. (5)).[24]

$$^{\circ}G\,(\mathrm{J\,mol^{-1}}) = -1\,976\,462 + 731.6512T - 121.881T \ln T - 0.005060T^2 + 1\,090\,000T^{-1} - 1.3 \times 10^7 T^{-2} \quad (5)$$

Preliminary thermodynamic calculations showed that YO_2 is the main Y-bearing gaseous species in equilibrium with α-Y_2O_3 in dry air. Partial pressures around 10^{-9} and 10^{-12} atm were respectively calculated at 1400 and at 1100 °C.

The system Y–O–H has not been yet investigated. The above-described procedure was then applied to estimate the Gibbs free energy of formation of yttrium hydroxide. For that purpose, the volatilisation rate of Y_2O_3 in a moist environment at high temperatures was determined. With respect to Eqs. (6) and (7), two gaseous species YOOH and $Y(OH)_3$ are formed when yttria is in contact with water vapor at high temperature.

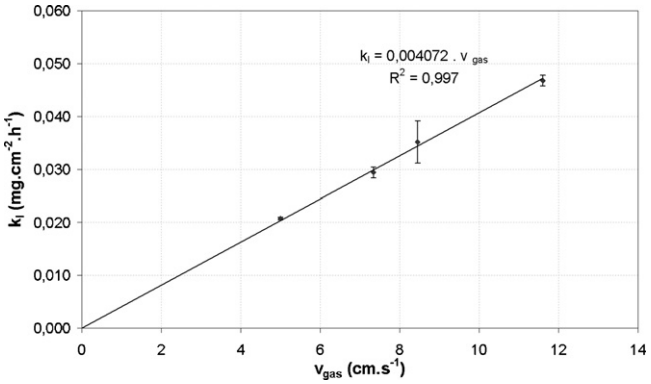

Fig. 4. Volatilisation rate of Y_2O_3 in function of gas velocity (under corrosion at 1200 °C, in air with 50 kPa H_2O, at P_{atm}) (if not visible, uncertainties are hidden in the size of the dots).

$$Y_2O_3 + 3H_2O \rightarrow 2Y(OH)_3 \quad (6)$$

$$Y_2O_3 + H_2O \rightarrow 2YOOH \quad (7)$$

First of all, it appears important to check that the thermodynamic equilibrium is always reached between this poorly known compound and the gaseous phase. According to Eq. (4), the linear dependence of the vaporization rate with the flow rate over the pellet was first checked. So the entrainment of the equilibrium vapor by convection remains the limiting step in the volatilisation process. Thus, volatilisation tests were carried out at 1200 °C in air with 50 kPa of water at atmospheric pressure, under different flowing gas velocities. The volatilisation rates were deduced from the slope of the experimental straight line corresponding to the weight loss/surface ratio as a function of time. Then, the values of rates were plotted in function of the gas velocity (Fig. 4). The proportionality relation is verified in the range of gas velocity considered. A straight line through the origin is obtained, as expected (Eq. (4)). The thermodynamic equilibrium appears to be reached whatever the gas velocity and the same value of partial pressure of the gaseous volatile species over Y_2O_3 is deduced from the slope. Consequently, in order to be at the thermodynamic equilibrium with convective flows and to limit the interaction with $Al(OH)_3$ from the furnace tube (whose formed quantities are logically proportional to the gas velocity), a working gas velocity of 5 cm s^{-1} is chosen.

Further, volatilisation tests are done at different temperatures in air with a water partial pressure of 50 kPa at atmospheric pressure under a gas velocity of 5 cm s^{-1}. The variations of the ratio between the weight change and the surface of the pellet as a function of time are shown at different temperatures in Fig. 5. The weight loss is linear with time and increases with temperature. The volatilisation rates k_l deduced from the slope of the linear curves (Fig. 5) are gathered in Table 1. Using an Arrhenius plot, the thermoactivation of the reaction of Y_2O_3 with moisture reveals a discontinuity at 1200 °C (Fig. 6). For temperatures below 1200 °C, the value of activation energy is around 41 ± 1 kJ mol^{-1}, against around 175 ± 10 kJ mol^{-1},

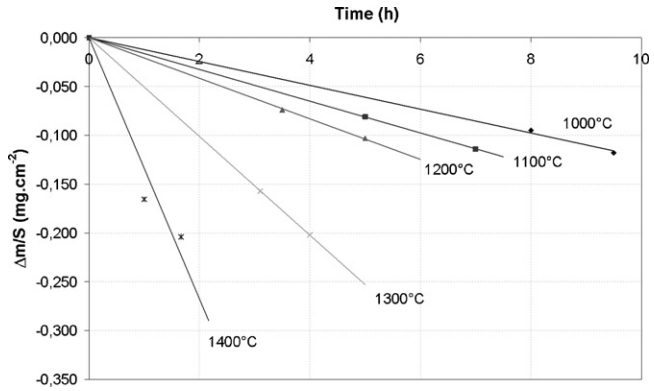

Fig. 5. Weight losses as a function of time during volatilisation of Y_2O_3 at different temperatures (under corrosion at 50 kPa H_2O, at P_{atm} with $v_{gas} = 5$ cm s^{-1}).

Table 1
Volatilisation rates of Y_2O_3 (determined for the following conditions: 50 kPa H_2O, P_{atm}, $v_{gas} = 5$ cm s^{-1}).

Temperature	k_l (mg cm^{-2} h^{-1})
1000 °C, 1273 K	0.0122 ± 0.0003
1100 °C, 1373 K	0.0162 ± 0.0001
1200 °C, 1473 K	0.0208 ± 0.0003
1300 °C, 1573 K	0.051 ± 0.001
1400 °C, 1673 K	0.12 ± 0.02

above 1200 °C. This last value is much higher than that corresponding to the volatilisation of silica (61 ± 8 kJ mol^{-1}).[12,19] At high temperatures (>1200 °C), yttrium hydroxides appear more difficult to form than $Si(OH)_4$.

This behaviour is indicative of a change in the volatilisation mechanism. Two domains of reactivity were thus assumed to take place according to temperature. They were associated with a change of the hydroxide species formed.

Now, it appears important to determine the nature of the different gaseous species, through experiments under various water vapor pressures. In fact, the (oxy-)hydroxides partial pressures depend on the water partial pressures according to Eqs. (6) and (7) (Eq. (8)). The (oxy-)hydroxide pressure $P_{M–OH}$, which corresponds to the sum of the partial pressures of YO_2, YOOH and

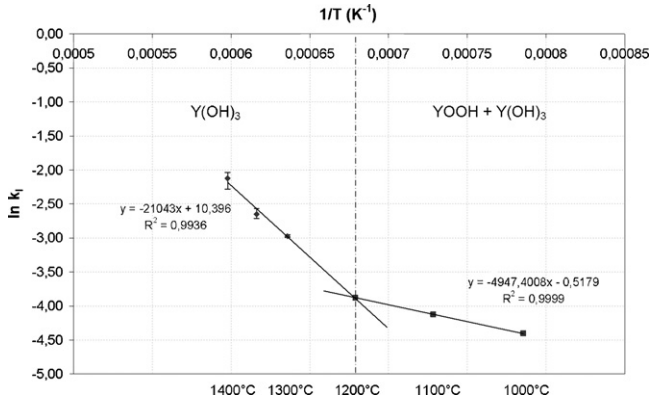

Fig. 6. Determination of the apparent kinetic laws of Y_2O_3 volatilisation by reaction with H_2O (with k_l in mg cm^{-2} h^{-1}) (uncertainties are in dots at low temperatures).

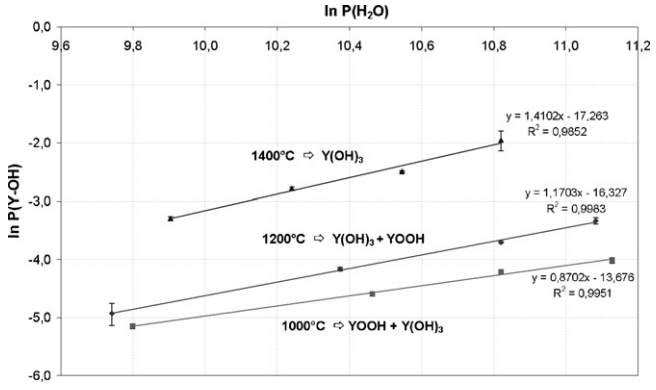

Fig. 7. Determination of the nature of the gaseous species at 1000, 1200 and 1400 °C through the extraction of the reaction order associated to H_2O (P_{atm}, $v_{gas} = 5$ cm s^{-1}) (with P in Pa) (if not visible, uncertainties are hidden in the size of the dots).

$Y(OH)_3$, is calculated from Eq. (4) and take into account the experimental gas flow velocity.

$$K = \frac{P_{M–OH}}{P_{H_2O}^{y}} \Rightarrow \ln P_{M–OH} = \ln K + y \ln P_{H_2O} \quad (8)$$

As a consequence, plotting $\ln P(Y–OH)$ versus $\ln P(H_2O)$, a slope equal to 1.5 is expected for the formation of $Y(OH)_3$ (Eq. (6)), whereas a slope equal to 0.5 would be obtained for the formation of YOOH (Eq. (7)).

Further volatilisation tests were carried out at different temperatures in air with different water partial pressures ranging from 17 to 65 kPa at atmospheric pressure, with a gas flow velocity of 5 cm s^{-1}. As expected, the yttria volatility rate increases in function of moisture content. Three different slope values equal to 0.87, 1.19 and 1.41 were respectively measured at 1000, 1200 and 1400 °C respectively (Fig. 7). From these results, formation of YOOH is expected to take place mainly at low temperature, whereas $Y(OH)_3$ should be the high temperature hydroxide species. Moreover, the slopes increase with temperature, that means that the proportion of $Y(OH)_3$ raises with temperature at the expense of YOOH. The change of the nature of the main volatile gaseous species (YOOH or $Y(OH)_3$) has to be related to the slope fracture shown in Arrhenius graph at 1200 °C (Fig. 6). For temperatures lower than 1200 °C, the predominant gaseous species is YOOH. For temperatures higher than 1200 °C, $Y(OH)_3$ becomes the major species. Moreover for temperatures upper than 1300 °C, $Y(OH)_3$ can be assumed to be the only volatile gaseous species since the partial pressure of YOOH is comparatively negligible.

6. Free energy of formation of yttrium (oxy-)hydroxides

The above-described approach based on the measurement of the partial pressures was used to determine the Gibbs free energy of formation of the yttrium hydroxides. These partial pressures are estimated from the apparent volatilisation kinetic law obtained with a water partial pressure of 50 kPa (Fig. 6 and Eq. (4)).

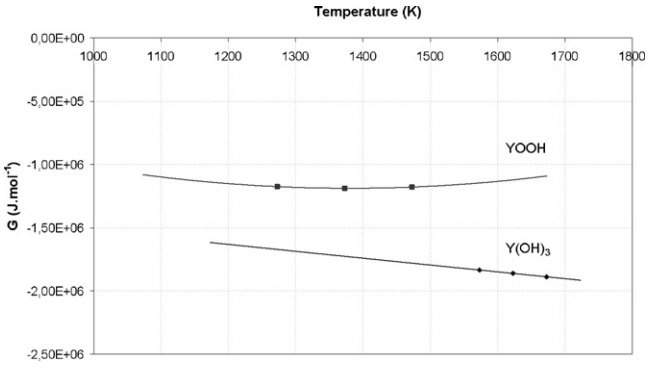

Fig. 8. Variation of the Gibbs free energy of formation of YOOH and $Y(OH)_3$ as a function of temperature.

In our study, two domains of temperature can be distinguished: the first one higher than 1300 °C, where $Y(OH)_3$ is the predominant species and the second one at temperatures lower than 1200 °C, where a mixture of YOOH and $Y(OH)_3$ is present. First the Gibbs free energy of formation of $Y(OH)_3$ is determined in the high temperature domain where two yttrium bearing species have to be considered: $Y(OH)_3$ and YO_2 (Eq. (9)). This last species is the predominant species formed in dry air atmosphere.

$$P_{exp} = P_{Y(OH)_3} + P_{YO_2} \quad (9)$$

The variations of Gibbs free energy of $Y(OH)_3$ formation between 1300 and 1400 °C were determined according to the above-described procedure from measurements of volatilisation rates carried out at 1300, 1350 and 1400 °C. A temperature dependent equation is extracted from the as determined date (Fig. 8). Extrapolation of this equation in the low temperature domain allowed to calculate the equilibrium partial pressures of $Y(OH)_3$ below 1300 °C. Consequently the equilibrium partial pressures of YOOH were deduced (Eq. (11)). The same procedure was applied at 1000, 1100 and 1200 °C and a temperature dependant equation was obtained in the low temperature domain (Fig. 8).

$$P_{exp} = P_{Y(OH)_3} + P_{YO(OH)} + P_{YO_2} \quad (10)$$

The temperature dependence equation of Gibbs free energy of formation of $Y(OH)_3$ and YOOH is respectively given by Eqs. (11) and (12):

$$\Delta G_{Y(OH)_3} = 1.1799999999 \times 10^{-2} T^2 - 5.756228 \times 10^2 T - 9.574324178 \times 10^5 \quad (11)$$

$$\Delta G_{YOOH} = 1.135 T^2 - 3.13381 \times 10^3 T - 9.75679715 \times 10^5 \quad (12)$$

Partial pressures of $Y(OH)_3$, YOOH and YO_2 in equilibrium with Y_2O_3 were then calculated by Gibbs free energy minimization (Fig. 9). Their variations are in agreement with the experimental observations, and confirm the negligible level of YOOH partial pressures in the range of temperatures upper than 1200 °C.

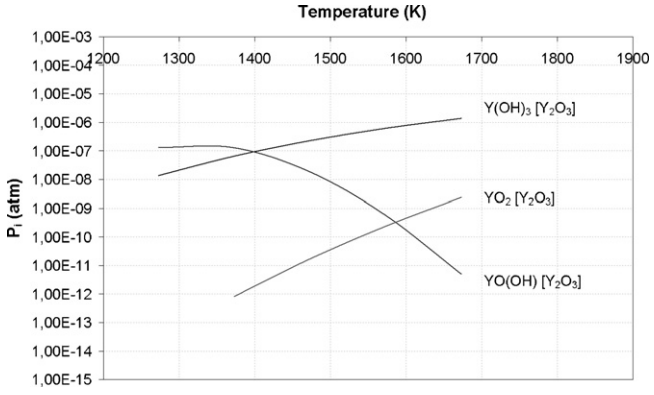

Fig. 9. Partial pressures of $Y(OH)_3$, YOOH and YO_2 over Y_2O_3 at equilibrium in a moist environment (calculated with the assessed thermodynamic data of $Y(OH)_3$ and YOOH) ($P_{Ar} = 40$ kPa, $P_{O_2} = 10$ kPa, $P_{H_2O} = 50$ kPa).

In order to check that the thermodynamic parameters are correct for different water partial pressures, the equilibrium Y-containing gaseous species partial pressures obtained experimentally (points) and those estimated by thermodynamic calculations (line) are compared at 1000, 1200 and 1400 °C for P_{H_2O} ranging from 17 and 65 kPa (Fig. 10). The good agreement between experience and theory allows validating our method and the accuracy of the assessed thermodynamic data.

7. Discussion

Moreover, these results can be compared with literature. By Krikorian,[29] the experimental and theoretical approaches were realised at high temperatures and at high pressure, 100 atm, in steam with a very low oxygen content, 10^{-2} atm. In such conditions, the considered main gaseous formed species over Y_2O_3 is $Y(OH)_3$. At high total pressure, the produced gaseous species always leads to a decrease of the total number of gaseous moles, as $Y(OH)_3$. Respectively, the theoretical predictive methods are developed for estimating the bond energies and free energy functions of volatile species, in order to extend knowledge of the mechanism and extent of steam-accelerated volatilisation

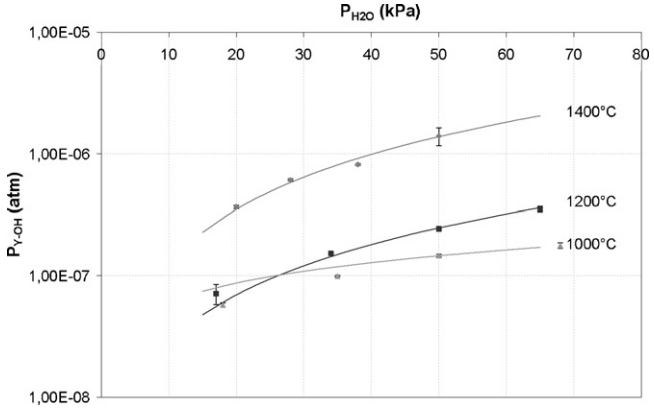

Fig. 10. Comparison of P(Y–OH) between calculations (line) (from assessed thermodynamic data) and experience (dots) from volatilisation tests at 1000, 1200 and 1400 °C under a moist environment ($P_{tot} = 100$ kPa, $v_{gas} = 5$ cm s^{-1}) (if not visible, uncertainties on the experimental results are hidden in the size of the dots).

processes. Using these data, the calculated hydroxides partial pressures are lower than those experimentally estimated from our experimental procedures. However, it is clearly mentioned by Krikorian that in most cases the combined presence of steam and oxygen gives rise to a greater increase in metal oxide volatility than the presence of steam alone.[29]

Through works about vapor transport of fission products under nuclear accident conditions by Cubicciotti,[30] the metal oxide volatility has been quantified in H_2O and H_2 gas flows, under high pressures, 3 and 170 atm, at high temperatures. In this work, only hydroxides species are again considered (no oxy-hydroxides). In the divers atmospheres characterized by different H_2/H_2O ratios, the hydroxide ($Y(OH)_3$) partial pressures remain much lower than those estimated in our conditions, with O_2/H_2O mixtures. In H_2/H_2O mixtures, these pressures depend not only the temperature but on the partial pressures of reactive gas, H_2 and H_2O, in the system.

Our work has not to be opposed to these results, but is a complement in oxidizing and moist environments. In this kind of environment, the mechanisms involved in the formation of oxy-hydroxides and hydroxides should be more complex.

8. Conclusion

The kinetics study of yttrium sesquioxide volatilisation in a moist environment enabled us: (i) to determine the activation energy of this reactive volatilisation, (ii) to identify the nature of the volatile (oxy-)hydroxides formed as a function of temperature and to propose a volatilisation mechanism in function of temperature, and (iii) to assess the Gibbs free energies of $Y(OH)_3$ and YOOH formation.

Further works will be devoted to the determination of the chemical and thermal stability of other rare earth oxides and then to the quantification of the stability of the Y_2O_3–SiO_2 and Y_2O_3–Al_2O_3 systems. This work will be used to understand the stability of yttrium silicates higher than silica. It will be proved that this higher stability is linked to the decrease of one magnitude order of the silica activity in yttrium silicates.

Acknowledgement

This work has been supported by the French Ministry of Education and Research through a grant given to E. Courcot.

References

1. Yano M, Tomita A, Sano M, Hibino T. Recent advances in single-chamber solid oxide fuel cells: a review. *Solid State Ionics* 2007;**177**:3351–9.
2. Cao XQ, Vassen R, Stöver D. Ceramic materials for thermal barrier coatings. *J Eur Ceram Soc* 2004;**24**:1–10.
3. Padture NP, Gell M, Klemens PG. Ceramic materials for thermal barrier coatings. US patent no. 6 015 630; 18 January 2000.
4. Lee KN, Fox DS, Bansal NP. Rare earth silicate environmental barrier coatings for SiC/SiC composites and Si_3N_4 ceramics. *J Eur Ceram Soc* 2005;**25**:1705–15.
5. Gu H, Chen H, Guo L. Effect of nano-Al_2O_3 and Y_2O_3 on the properties and microstructure of Si_3N_4. *Mater Sci Eng A* 2008;**491**:177–81.
6. Meschi DJ, Chupka WA, Berkovitz J. Heterogeneous reactions studied by mass spectrometry. I. Reaction of B_2O_3 (s) with H_2O (g). *J Chem Phys* 1960;**33**:530–3.
7. Berkovitz J, Meschi DJ, Chupka WA. Heterogeneous reactions studied by mass spectrometry. I. Reaction of Li_2O (s) with H_2O (g). *J Chem Phys* 1960;**33**:533–40.
8. Murad E. Thermochemical properties of gaseous FeO and FeOH. *J Chem Phys* 1980;**73**:1381–5.
9. Hildenbrand DL, Lau KH. Thermochemistry of gaseous SiO(OH), $SiO(OH)_2$ and SiO_2. *J Chem Phys* 1994;**101**:6076–9.
10. Hildenbrand DL, Lau KH. Comments on thermochemistry of gaseous SiO(OH), $SiO(OH)_2$ and SiO_2. *J Chem Phys* 1998;**108**:6535.
11. Hildenbrand DL, Lau KH. Thermochemistry of gaseous manganese oxides and hydroxides. *J Chem Phys* 1994;**100**:8377–80.
12. Hashimoto A. The effect of H_2O gas on volatilities of planet-forming major elements: I. Experimental determination of thermodynamic properties of Ca-, Al-, and Si-hydroxide gas molecules and its application to the solar nebula. *Geochim Cosmochim Acta* 1992;**56**:511–32.
13. Ali (Basu) M, Mishra R, Kerkar AS, Bharadwaj SR, Das D. Gibbs energy of formation of $Ba(OH)_2$ vapor species using the transpiration technique. *J Nucl Mater* 2001;**289**:243–6.
14. Jacobson NS, Opila EJ, Myers DL, Copland EH. Thermodynamics of gas phase species in the Si–O–H system. *J Chem Thermodyn* 2005;**37**:1130–7.
15. Opila EJ, Myers DL. Alumina volatility in water vapor at elevated temperatures. *J Am Ceram Soc* 2004;**87**:1701–5.
16. Allendorf MD, Besmann TM. Thermodynamics resource (Sandia National Laboratory database). http://public.ca.sandia.gov/HiTempThermo.
17. Quémard L, Rebillat F, Guette A, Tawil H, Louchet-Pouillerie C. Degradation mechanisms of a SiC fiber reinforced self sealin matrix composite in simulated combustor environments. *J Eur Ceram Soc* 2007;**27**:377–88.
18. Association Thermodata GEMINI 2 Code. B.P. 66, 38402 St. Martin d'Heres Cedex, France.
19. Opila EJ, Hann Jr RE. Paralinear oxidation of CVD SiC in water vapor. *J Am Ceram Soc* 1997;**80**:197–205.
20. Liu MN, Wahlbeck PG. Knudsen effusion and mass spectrometric studies of the vaporization of Y_2O_3(s). Dissociation energy of YO(g). *High Temp Sci* 1974;**6**:179–89.
21. Ackermann RJ, Rauh EG, Walters RR. Thermodynamic study of the system yttrium + yttrium sesquioxide. A refinement of the vapor pressure of yttrium. *J Chem Thermodyn* 1970;**2**:139–49.
22. Ames LL, Walsch PN, White D. Rare earths. IV. Dissociation energies of the gaseous monoxides of the rare earths. *J Phys Chem* 1967;**71**:2707–18.
23. Ackermann RJ, Rauh EG, Thorn RJ. Thermodynamic properties of gaseous yttrium monoxide. Correlation of bonding in group III transition-metal monoxides. *J Chem Phys* 1964;**40**:883–9.
24. Djurovic D, Zinkevich M, Aldinger F. Thermodynamic modeling of the yttrium–oxygen system. *Comp Coupling Phase Diag Thermochem* 2007;**31**:560–6.
25. Ran Q, Lukas HL, Henig ET, Effenberg G, Petzow G. Optimization and calculation of the Y–O system. *Z Metallkd* 1989;**80**:800–5.
26. Gröbner J, Kolitsch U, Seifert HJ, Fries SG. Re-assessment of the Y–O binary system. *Z Metallkd* 1996;**87**:88–91.
27. Lysenko VA. Thermodynamic calculation of the yttrium–oxygen phase diagram. *Inorg Mater* 1996;**32**:392–6.
28. Swamy V, Seifert HJ, Aldinger F. Thermodynamic properties of Y_2O_3 phases and the yttrium–oxygen phase diagram. *J Alloys Compd* 1998;**269**:201–7.
29. Krikorian OH. Predictive calculations of volatilities of metals and oxides in steam-containing environments. *High Temp – High Press* 1982;**14**:387–97.
30. Cubicciotti D. Vapor transport of fission products under nuclear accident conditions. *J Nucl Mater* 1988;**154**:53–61.